J. Membrane Biol. 72, 195–203 (1983)

The Journal of
Membrane Biology

Ionic Currents in Cultured Dorsal Root Ganglion Cells from Adult Guinea Pigs

Masaki Kameyama
Department of Physiology, Faculty of Medicine, University of Tokyo, Tokyo 113, Japan

Summary. Ionic currents in cultured dorsal root ganglion (DRG) neurons from *adult* guinea pigs were analyzed by voltage-clamp techniques. The Na^+ inward current had a reversal potential at +33 mV, and revealed activation and inactivation kinetics similar to those of squid giant axons. A typical value for the maximum Na^+ conductance was 178 mS/cm^2 and the peak current was 2.5 mA/cm^2. The delayed K^+ outward current showed a fast and a slow phase of inactivation and was sensitive to tetraethylammonium (TEA; ~130 mM) and 4-aminopyridine (~2 mM). The maximum K^+ conductance was 26 ± 9 (mean $\pm$ SD) mS/cm^2. The slow Ca^{2+} inward current was identified in Na^+-free, TEA-containing solution. Its peak value was increased by 1.7-fold when $[Ca^{2+}]_o$ was increased from 5 to 10 mM. The current was blocked by Co^{2+} but not by tetrodotoxin. Sr^{2+} and Ba^{2+} could substitute in carrying this current. The maximum peak of the Ca^{2+} current was 0.22 ± 0.14 mA/cm^2. At potentials positive to 0 mV, the Ca^{2+} current was often followed by a slowly developing outward current, which was also sensitive to Co^{2+}, suggesting a Ca^{2+}-activated outward current. It is concluded that the action potential of the *adult* guinea pig DRG neuron is mediated by Ca^{2+} as well as by Na^+ and K^+ currents. The current densities of these ionic channels are considered to be different from *embryonic* neurons and from nodes of Ranvier.

Key Words cell culture · dorsal root ganglion · voltage clamp

Introduction

Our knowledge of the excitability mechanisms of nerve cell bodies, especially concerning their ionic basis, derives mostly from experiments on invertebrate neurons. The Ca^{2+} current as well as the Na^+ and K^+ currents are involved in the formation of the action potentials (for review, *see* Hille, 1977). Until recently, however, little was known about the ionic current mechanisms of the action potentials of mammalian nerve cell bodies. Recent studies on *embryonic, neonatal* and *neoplasmatic* mammalian nerve cells have demonstrated that the ionic mechanisms of the excitability in such cell bodies are basically identical to those in invertebrate neurons (Matsuda, Yoshida & Yonezawa, 1976, 1978; Moolenaar & Spector, 1977, 1978, 1979; Ransom & Holz, 1977; Kostyuk, Veselovsky & Fedulova, 1981; Kostyuk, Veselovsky, Fedulova & Tsyndrenko, 1981; Kostyuk, Veselovsky & Tsyndrenko, 1981). Previous voltage-clamp experiments on *adult* mammalian neurons have also revealed a fast Na^+ current and a fast and a slow K^+ current, but have provided few indications of the existence of an additional slow inward current carried by Ca^{2+} (Barrett, Barrett & Crill, 1980; Barrett & Crill, 1980).

The results of the present study demonstrate that *adult* mammalian nerve cells have a well-defined Ca^{2+} inward current in addition to the Na^+ and K^+ currents. The properties of these current systems are essentially similar to those in *embryonic, neonatal* and *neoplasmatic* mammalian nerve cells. At the same time, some differences in the ionic mechanisms of the excitability of the *adult* nerve cell bodies from the *embryonic* (or *neoplasmatic*) nerve cell bodies and from nerve fibers were found.

Present address: National Institute for Physiological Sciences, Myodaijo-cho, Okazaki 444, Japan.

Materials and Methods

Nerve Cell Culture

The procedure of cell culture was essentially the same as that described previously (Fukuda & Kameyama, 1979, 1980*a, b*). Dorsal root ganglion (DRG's) from adult guinea pigs weighing 250 to 350 g, were dissected out and minced into blocks measuring 0.5 mm. The nerve cells were dissociated with collagenase (0.3 to 0.5%; Boehringer) in L-15 medium (Flow Lab., U.S.A.) for 30 to 60 min at 37 °C. The cells so obtained were plated in culture medium in collagen-coated plastic dishes (35 mm in diameter; Lux, U.S.A.) at a density of approximately 3×10^4 nerve cells per dish and were incubated at 37 °C in humidified air containing 5% CO_2. The culture medium contained 75% Eagle's minimum essential medium (Microbiol. Assoc. U.S.A.),

15% horse serum (same origin) inactivated by heat (60 °C for one hour), 9% chick embryo extract (homemade) and 1% penicillin-streptomycin solution (GIBCO, U.S.A.). The culture medium was changed 2 to 3 times a week.

Voltage Clamp

Nerve cells after 2 to 4 days in culture, having diameters of 30 to 70 μm with short or no neurite(s), were used for the electrophysiological experiments. A culture dish was mounted on the stage of an inverted phase-contrast microscope (Olympus, Japan). Cells were impaled with two glass microelectrodes (30 to 60 MΩ) filled with 3 M KCl or 2 M K-citrate solution. To minimize the coupling capacitance, the two microelectrodes were shielded with aluminium foil and a grounded shield was placed between them.

The voltage-clamp techniques used were essentially similar to those described elsewhere (Fukuda, Fischbach & Smith, 1976). The time resolution of the voltage clamp was significantly improved by modifying the clamp amplifier according to the procedure of Smith et al. (1980). The amplifier has complex gain-frequency characteristics: from 0 Hz to about 1 Hz the gain is high ($\sim 10^5$), and decreases by 20 dB/decade up to a relatively low gain ($\sim 10^3$) region from about 100 Hz to 700 kHz. In the optimal condition, the potential change in response to a 10-mV hyperpolarizing step was 90% complete within 200 to 300 μs in cells without neurites (e.g. Fig. 2*A* below). In experiments on the slow inward current, electrodes with relatively high resistance were necessary for stable recording of the current due to its labile nature. Under such conditions, although the capacitative current usually lasted 1 to 2 msec, this time was sufficiently short to analyze the activation time course of the slow inward current. The membrane current was measured with a current-to-voltage converter through a 3 M KCl-agar bridge. The first derivative of the membrane potential was obtained with an analog differentiator (time constant, 0.1 ms). All signals were displayed on a CRT and were photographed for later analysis.

The surface area of the nerve cell body (S) was calculated by assuming a hemi-ellipsoid shape (*see* Fig. 7 in Ransom et al., 1977) as $S = 3\pi \times$ (long axis) $\times$ (short axis)/4 for estimation of the membrane current density.

Space Clamp

In the voltage-clamp experiments, the soma membranes of the cells were adequately space clamped since the configuration of action potentials recorded from the two electrodes was identical. Furthermore, analysis of the cable parameters (Rall, 1969) of neurites of the cells after 2 to 3 days in culture revealed that the electrotonic length (the length of the neurite in terms of the length constant) was less than 0.5, and that the conductance ratio of the neurite to the soma was too small to be determined. However, in the experiments on the fast inward current, "abominable notches" in the inward current, an indication of an incomplete space clamp (Cole, 1968), were often seen. It was necessary therefore to select cells without neurites, so that the experiments on the fast inward current were carried out only in cells after 2 days in culture.

Series Resistance

A small resistance of 20 kΩ in series with the membrane resistance (15 to 50 MΩ) was measured under constant-current conditions. The error associated with measurement of the membrane potential in voltage-clamp experiments due to the series resistance was less than 4 mV, since the ionic currents measured in the experiments were less than 200 nA. Thus, the error of the measured potential could be safely neglected and no compensation was considered.

Bathing Solutions

The cells were bathed either in L-15 medium or in salt solutions. The normal salt solution consisted (in mM) of NaCl 153, KCl 5.5, $CaCl_2$ 2.0, glucose 5.5 and Na-Hepes 2.0, and the pH was adjusted to 7.4. In Na^+-free solutions, Tris-HCl was isosmotically substituted for NaCl and Na-Hepes. Further modifications of the ionic composition were carried out keeping the tonicity equal, except that tetrodotoxin (TTX, 3×10^{-6} M; Sankyo, Japan) was simply added to the solutions. Co^{2+} (1 to 10 mM) was employed as a Ca^{2+} current blocker. The outward currents were blocked by both tetraethylammonium (TEA; 10 to 140 mM) and 4-aminopyridine (4-AP; 0.5 to 2 mM).

The temperature of the bathing solution was controlled at between 17 and 27 °C using a thermoelectric module.

Results

General Properties

The cultured cells employed in this study had resting potentials of between −35 and −60 mV, membrane input resistances of around 25 MΩ and input capacitances of around 80 pF. Figure 1*A* illustrates the regenerative action potential in a Na^+-solution containing 1 mM Co^{2+}. The threshold, overshoot and maximum rate of rise ($\dot{V}_{max}$) of the action potential were −35 mV, 31 mV and 136 V/sec, respectively. The potential response to the hyperpolarizing current revealed the membrane time constant of 2.4 msec and an additional slow component (time constant, 18.3 ms), with no indication of inward rectification. The action potential was abolished in Na^+-free solutions, but a slow active response could be elicited when TEA (50 mM) was substituted for equimolar Tris (Fig. 1*B*). The threshold (−32 mV) and overshoot (27 mV) of such an action potential were close to the corresponding values for the Na^+-dependent spike in Fig. 1, but the duration of the action potential (160 ms) was 80 times longer, and $\dot{V}_{max}$ (29 V/sec) was about 5 times smaller than for the Na^+-spike. This slow response was abolished by the application of 5 mM Co^{2+} to the bathing solution. These results confirmed our previous studies suggesting that Na^+, K^+ and Ca^{2+} channels are involved in the formation of the action potential in cultured DRG cells (Fukuda & Kameyama, 1979, 1980*b*).

The Fast Inward Current

An inward current, activated at potentials positive to −28 mV, could be consistently recorded in the

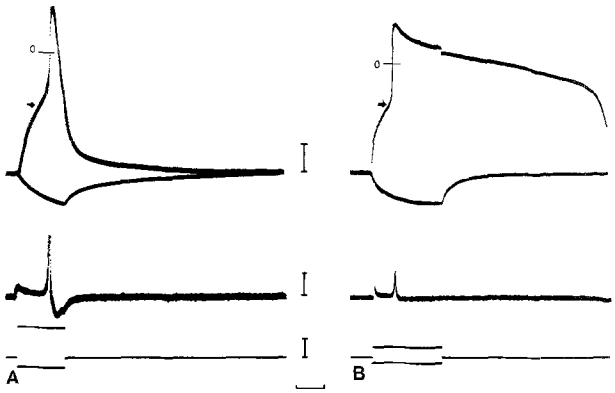

Fig. 1. Electrical responses of cultured DRG neurons under constant current conditions. (*A*) Evoked responses of a cell after 3 days in culture in a solution containing (in mM) NaCl 143, TEA-Cl 10, KCl 5.5, $CaCl_2$ 1.0, $CoCl_2$ 1.0, glucose 5.5 and Na-Hepes 2.0. Upper traces, evoked membrane responses; middle traces, first derivative of the action potential; lower trace, intracellularly applied currents. Short bars with 0 indicate the reference potential. Arrows indicate the threshold of the action potential. (*B*) Responses of a cell after 4 days in culture in Na^+-free solution with 10 mM Ca^{2+}, 50 mM TEA and 2 mM 4-AP. Traces are as in *A*. Calibrations: *A*, 20 mV, 60 V/s, 1 nA, 5 ms; *B*, 20 mV, 30 V/s, 1 nA, 20 ms

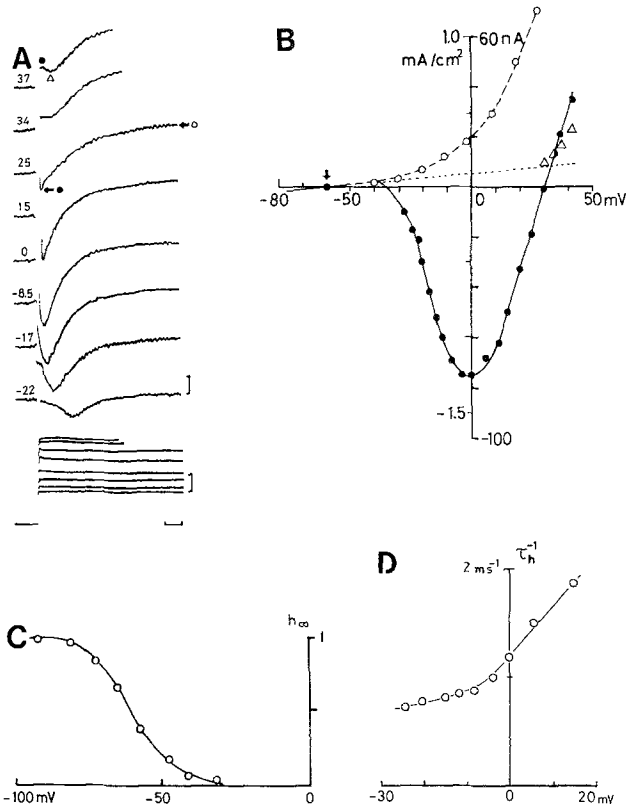

Fig. 2. Na^+ current under voltage clamp in a DRG cell after 2 days in culture. (*A*) Family of current traces and superimposed potential traces in L-15 medium. Numbers indicate the test potentials in mV. Calibration: 20 nA, 20 mV, 1 ms. (*B*) *I–V* relations of the peak current (•), current at 1 ms (*Δ*) and at 9.5 ms (○) after onset of the test pulses as shown in *A*. Dotted line, linear leak current line. Cell size: 59 × 43 μm. Temp.: 20 °C. Arrow indicates the holding potential in Figs. 2 to 9. (*C*) Steady-state inactivation (h_∞) of I_{Na}. (*D*) Inactivation rate constant (τ_h^{-1}) of I_{Na} against membrane potential (V_m). τ_h^{-1} was obtained from the slope of the straight line in semi-logarithmic plots of current against time

Na^+-containing solutions. This current became inactivated rapidly and was followed by a delayed outward current (Fig. 2*A*). Figure 2*B* shows the current-to-voltage (*I–V*) relation of both the inward and outward currents. The maximum value of the inward current was 1.25 mA/cm² at 0 mV when the membrane potential was held at −60 mV. The *I–V* curve intersects the linear leak current line at 33 mV, close to the Nernstian equilibrium potential for Na^+ ($E_{Na} = 40$ mV at 20 °C, assuming $[Na^+]_i = 30$ mM). At potentials positive to 34 mV, the fast inward current clearly reversed as is evident in the current trace in Fig. 2*A*. The fast inward current was abolished in Na^+-free solutions (*see* inset of Fig. 3*A*). TTX reduced this current to about 20% of its control value. The results suggest therefore that the fast inward current is carried mainly by Na^+ (I_{Na}).

The steady-state inactivation (h_∞) of I_{Na} was examined by applying a prepulse (−95 to −33 mV) about one second prior to a test pulse of −10 mV (Fig. 2*C*). The continuous curve in Fig. 2*C* is drawn according to the equation, $h_\infty = 1/(1+\exp(V_m - V_h)/K_h)$, where $V_h = 60$ mV and $K_h = 7.0$ mV. The decay phase of I_{Na} fits well with single exponential lines in the potential range of from −25 to −6 mV, where the activation of the delayed outward current is slow and small compared to the inactivation of the fast inward current. The inactivation time constant (τ_h), as determined from the slope of the fitted lines, is shown in its reciprocal form (inactivation rate) in Fig. 2*D*. It should be noted that the inactivation rate was accelerated with depolarization of the membrane potential, between −25 and 15 mV.

In the case of the cell illustrated in Fig. 2, the activation kinetics of I_{Na} were analyzed at membrane potentials of between −25 and −8 mV, using the Hodgkin-Huxley formulation by assuming the activation parameter as m^3. In this potential range the time to peak was more than 0.6 msec. The time constant of the activation was between 0.81 (−25 mV) and 0.16 msec (−8 mV), decreasing monotonically with depolarization. The maximum conductance ($\bar{g}_{Na}$) and the maximum value of the peak I_{Na} were calculated as 178 mS/cm² and 2.5 mA/cm², respectively.

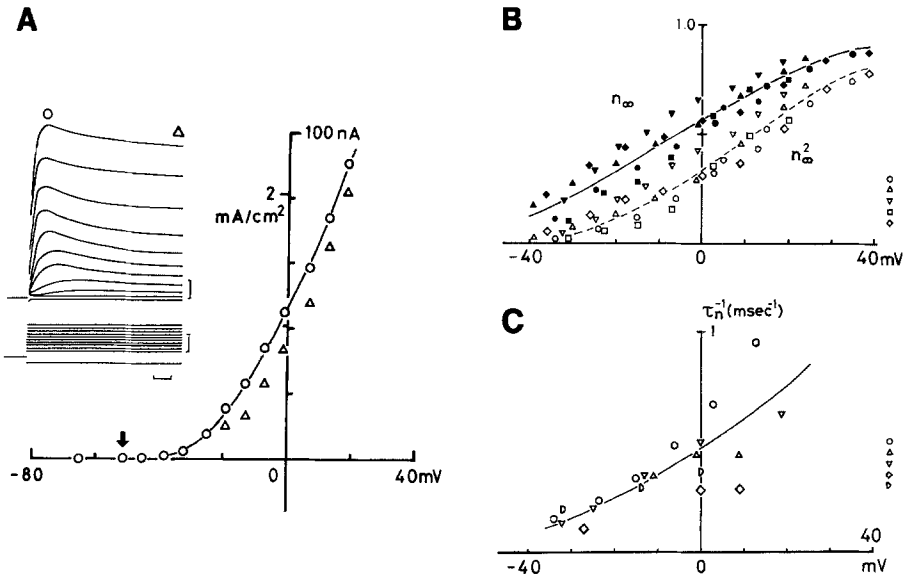

Fig. 3. Delayed outward current and its kinetics. (*A*) *I–V* relation of a cell after 3 days in culture in Na^+-free solution with 10 mM Co^{2+}. o, peak outward current; Δ, current at 80 ms after onset of the test pulse. The linear leak current was subtracted. Cell size: 44 × 39 μm. Temp.: 20 °C. Inset shows superimposed current and voltage traces. Calibration: 10 nA, 50 mV, 10 ms. (*B*) n_∞^2 (open symbols) and n_∞ (filled symbols) in 5 cells. $\bar{g}_K n_\infty^2$ (steady state g_K corrected for inactivation) was obtained by extrapolation of the current to time zero. g_K was determined from the asymptote of the log $\bar{g}_K n_\infty^2$ vs. V_m plot. Temp.: 20 to 26 °C. (*C*) τ_n^{-1} in 5 cells. τ_n^{-1} was obtained from the slope of the semi-logarithmic plot of $\sqrt{\bar{g}_K n_\infty^2 h} - \sqrt{g_K}$ against time, assuming $n_\infty = 0$ at potentials negative to −50 mV. Temp.: 26 °C for o; 20 °C for others. The lines in *A–C* were fitted by eye

The Delayed Outward Current

The outward current was analyzed in Na^+-free solutions with 10 mM Co^{2+} in which the inward current components were entirely eliminated. The *I–V* relation of the outward current rectified at potentials positive to −40 mV (Fig. 3*A*). The inset in Fig. 3*A* illustrates a superimposed current trace of the outward current with various test pulses, in which the outward current induced by depolarization decayed with a slow time course. The peak current value of the outward current ranged from 0.34 to 1.11 (average 0.57) mA/cm² at 0 mV in 8 cells, with holding potentials of between −51 and −64 mV.

The K^+ dependency of the outward current was examined by measuring the reversal potential of the tail current which was induced by the cessation of 20 ms depolarizing pulses at various $[K^+]_o$. The reversal potentials at $[K^+]_o$ of 5.5, 18 and 55 mM were −77 (5 cells), −48 (5 cells) and −18 mV (2 cells), respectively, which corresponds to a 58-mV change of reversal potential with a 10-fold increase in $[K^+]_o$. The delayed outward current is thus carried predominantly by K^+ (I_K).

The time course of the decay of I_K consisted of two exponential components, a fast and a slow phase. The time constant varied from cell to cell, being 10 to 50 ms for the fast and 150 to 1500 ms for the slow phase, at 0 mV in 5 cells. In a typical example with a holding potential of −78 mV, the two time constant values were 11 and 480 ms, at 0 mV and 26 °C. The activation phase of the outward current was analyzed according to the Hodgkin-Huxley model. From the slope of double logarithmic plots of I_K versus time, the best fit for the exponent of the n variable resulted at 2. The maximum K^+ conductance ($\bar{g}_K$) was 26.1 ± 8.9 mS/cm² in 5 cells (*see* legend to Fig. 3*B*). The steady-state value of n (n_∞) was 0.5 at about −10 mV and the time constant of n (τ_n) was 2.5 ms at 0 mV (Fig. 3*B, C*).

Both TEA and 4-AP produced a marked reduction of the outward current (Fig. 4). In TEA solution, both the activation and inactivation kinetics appeared to be unaffected, whereas in 4-AP solution both were significantly slowed.

The Slow Inward Current

An inward current underlying the slow action potential in Na^+-free solutions containing TEA and 4-AP was activated by depolarizing pulses positive to −30 mV (holding potential of −80 mV) as illustrated in Fig. 5*A*. The maximum peak for this current appeared at a potential of about −2 mV (Fig. 5*B*). The time course of this inward current

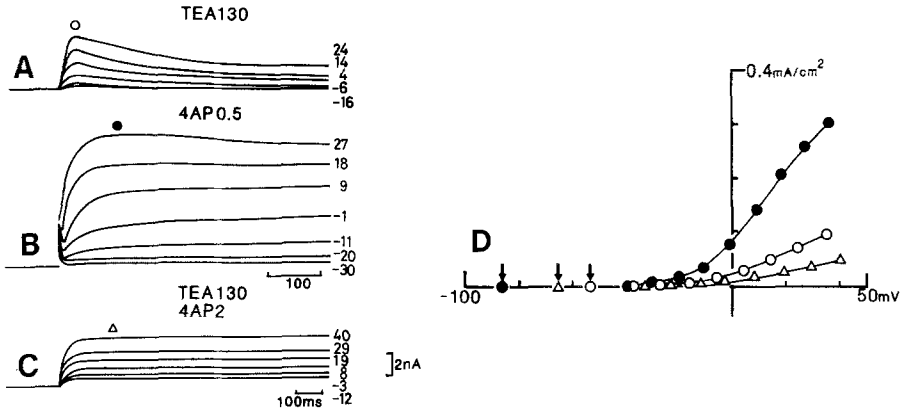

Fig. 4. Effect of TEA and 4-AP on I_K. (*A–C*) Superimposed current traces in 130 mM TEA (*A*), 0.5 mM 4-AP (*B*) and 130 mM TEA+2 mM 4-AP (*C*) solutions in different cells. Numbers indicate test potentials in mV. (*D*) *I–V* relation for *A* (○), *B* (●) and *C* (△). Note the marked reduction of I_K compared to I_K in Fig. 4*C*. Temp.: 20 to 26 °C

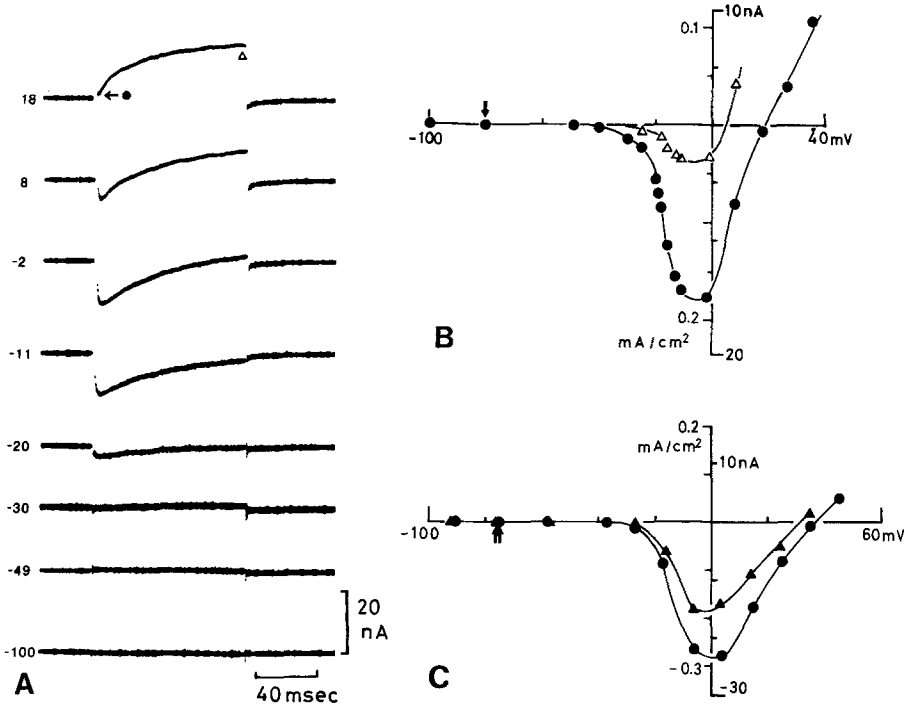

Fig. 5. Slow inward current and its Ca^{2+} dependency. (*A*) Current traces in Na^+-free solution with 10 mM Ca^{2+}, 50 mM TEA and 2 mM 4-AP in a cell after 3 days in culture. 100 ms test pulses were applied at an interval of 30 sec to avoid cumulative inactivation. Numbers indicate test potentials in mV. (*B*) *I–V* relation for the cell in *A*. ●, peak current; △, current at end of test pulse. Cell size: 62 × 58 μm. Temp.: 25 °C. (*C*) *I–V* relation in another cell after 3 days in culture. ▲, peak inward current in 5 mM Ca^{2+} + 5 mM Mg^{2+} solution; ●, that in 10 mM Ca^{2+} solution. The linear leak current was subtracted. Note the 1.6-fold increase in I_{Ca}. Cell size: 66 × 54 μm. Temp.: 17 °C

was much slower than that of I_{Na}. For example, at −2 mV, the slow inward current reached its peak value at 5 ms, whereas I_{Na} attained its peak at 0.5 ms. The slow inward current also became inactivated, but with a slower time course than that for I_{Na}. The slow inward current was found to depend on $[Ca^{2+}]_o$. Its peak value increased from 0.18 mA/cm² in 5 mM Ca^{2+} to 0.28 mA/cm² in 10 mM Ca^{2+} solution in the cell illustrated in Fig. 5*C* (average 1.7-fold increase in 3 cells).

After application of Co^{2+} (approximately 5 mM), this Ca^{2+}-dependent current (I_{Ca}) was abolished, leaving a residual outward current (Fig. 6*A, B*) which was essentially the same current as in Fig. 4. Figure 6 illustrates several other features of the membrane current in a Na^+-free solution, as follows. (1) In Co^{2+}-containing solution, the outward current elicited at potentials positive to 0 mV was reduced, indicating that there was a Co^{2+}-sensitive outward current as well as the Co^{2+}-resistant K^+ outward current. However, the magnitude of the Co^{2+}-sensitive outward current varied widely from cell to cell. (2) Reversal of I_{Ca} could not be observed although the *I–V* relation for I_{Ca} intersected the voltage axis at 10 mV. (3) I_{Ca} was not completely inactivated at the end of test pulses of between −40 and −10 mV (*see also* Figs. 5*A*, 7*A* and 8), lasting for as long as one second in some other cells. The long-lasting inward current may be responsible for the long-lasting plateau phase of the Ca^{2+}-dependent spike in Fig. 1*B*.

When Ca^{2+} was replaced with equimolar Sr^{2+}

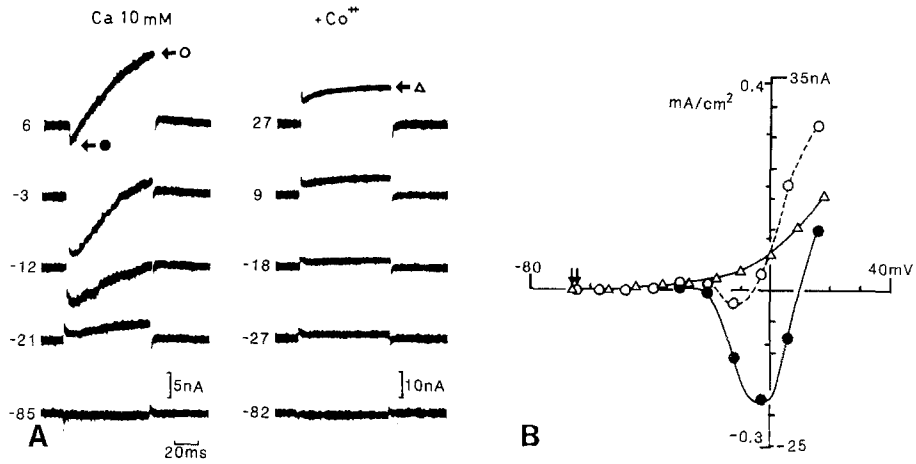

Fig. 6. Blocking effect of Co^{2+} on I_{Ca}. (*A*) Current traces in 10 mM Ca^{2+}, 50 mM TEA and 2 mM 4-AP without Co^{2+} (left column) and with Co^{2+} of approximately 5 mM (right column) in a cell after 2 days in culture. The pulse potential is indicated. (*B*) *I–V* relation for the cell in *A*. ●, peak current; current at end of test pulse without Co^{2+} (o) and with Co^{2+} (*Δ*). The leak current was subtracted. Cell size: 60 × 60 μm. Temp.: 26 °C

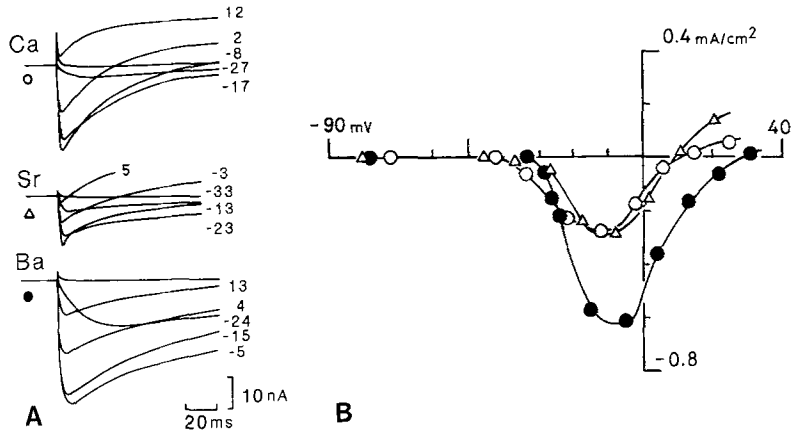

Fig. 7. Inward Ca^{2+}, Sr^{2+} and Ba^{2+} currents. (*A*) Superimposed current traces in 10 mM Ca^{2+} (upper), Sr^{2+} (middle) and Ba^{2+} (lower) solutions containing 50 mM TEA and 2 mM 4-AP. The leak currents were subtracted. The pulse potential is indicated. (*B*) *I–V* relation of the Ca^{2+} (o), Sr^{2+} (*Δ*) and Ba^{2+} (●) currents shown in *A*. Temp.: 26 to 27 °C

or Ba^{2+}, a similar slow inward current could be observed (Fig. 7). In Ba^{2+} solution, the amplitude of the current was larger and the time course of the current decay was slower than those of I_{Ca}. The maximum values of the peak current densities in 10 mM Ca^{2+}, Sr^{2+} and Ba^{2+} solutions were $0.22+0.21$ (mean+SD, 11 cells), 0.25 ± 0.03 (3 cells) and 0.40 ± 0.21 mA/cm^2 (5 cells), respectively. These currents were not affected by the application of 3 μM TTX.

The kinetics of I_{Ca} were analyzed by analogy to I_{Na} in cells, which demonstrated a small, slowly developing outward current as regarding its amplitude, in solutions containing both TEA (50 to 130 mM) and 4-AP (2 mM). In such cells, I_{Ca} could be analyzed without significant error at least at potentials negative to 10 mV, since in this potential range the activation of the outward currents was slower and smaller than at more positive potentials. The steady-state inactivation curve (Fig. 8*A*) showed a sigmoidal relationship, with $V_h = -38$ mV (-43, -38 and -33 mV in 3 cells) and $K_h = 8.7$ mV (8.5, 8.7 and 8.8 mV in 3 cells). The value of V_h was 22 mV more positive and the value of K_h was 1.2-fold larger than the corresponding values for I_{Na}. The time constant of the current decay (τ_h), shown in its reciprocal form in Fig. 8*A*, was 30 to 130 times larger than that for I_{Na} at test potentials of between -30 and 10 mV. With longer test pulses (up to one second), a slower inactivation phase following the initial phase could be observed in some cells. The time constant of the slow phase ranged from 210 to 650 ms at 0 mV in 5 cells.

The activation kinetics of I_{Ca} were analyzed well for its relatively slow time course. The time to peak of the current usually exceeded 5 ms at a potential negative to 0 mV. In the analysis of the activation kinetics, it was assumed that Ca^{2+} was the only permeant ion and that $[Ca^{2+}]_i$ was 10^{-7} M, giving a value of 150 mV for the equilibrium potential. The exponent of the activation variable was taken as unity, since exponents one and two fitted the experimental data equally well. The steady-state activation curve of I_{Ca} (Fig. 8*B*) revealed half activation at about -20 mV. The acti-

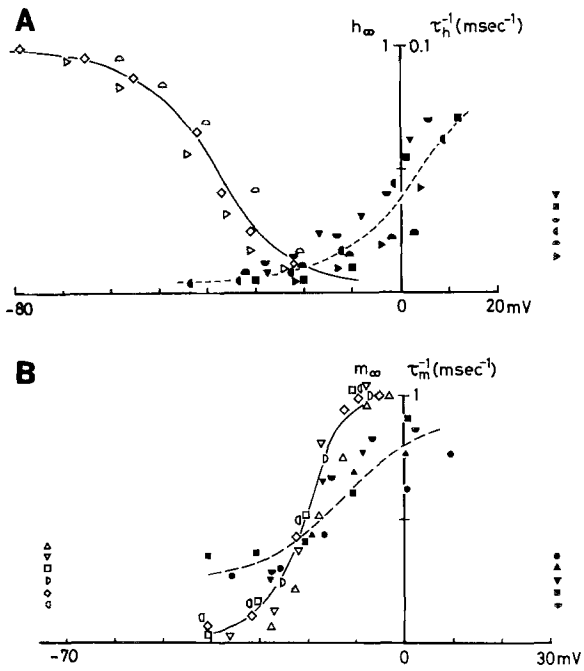

Fig. 8. Kinetic parameters for I_{Ca}. (*A*) h_∞ (open symbols, 3 cells) and τ_h^{-1} (filled symbols, 6 cells) against membrane potential. The curve for h_∞ is drawn according to $h_\infty = 1/(1+(V_m+38)/8.7)$. (*B*) m_∞ (open symbols, 6 cells) and τ_m^{-1} (filled symbols, 5 cells). Note the overlap of the steady-state activation and inactivation curves between -40 to -10 mV. Temp.: 17 to 27 °C for *A* and *B*. The lines for m_∞, τ_m^{-1} and τ_h^{-1} were fitted by eye

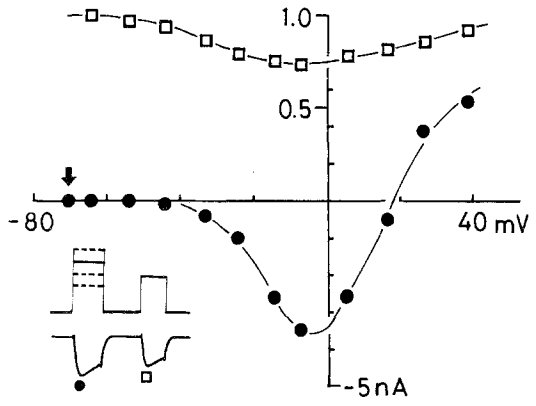

Fig. 9. Effect of preceding pulse on I_{Ca}. A conditioning pulse of variable amplitude and 100-ms duration was applied before the test pulse of -7 mV at an interval of 125 ms (shown schematically in the inset) in Na^+-free solution with 10 mM Ca^{2+}, 130 mM TEA, 2 mM 4-AP and 3 μM TTX. The peak I_{Ca} during the test pulse (●) and the normalized amplitude of the current during the test pulse (□) are plotted against the potential of the conditioning pulse. Temp.: 18 °C

vation time constant (τ_m) is plotted in Fig. 8*B* as τ_m^{-1}. The activation rate for I_{Ca} was about 16 times slower than that for I_{Na} at 0 mV.

The effect of Ca^{2+} entry on the Ca^{2+} conductance, as examined by the double-pulse method, is illustrated in Fig. 9. The peak I_{Ca} produced by the test pulse decreased as the current associated with the conditioning pulse increased, and vice versa. This suggests the existence of a Ca^{2+}-dependent inactivation process. However, the amount of inactivation caused by the conditioning pulse was much smaller than that observed in *Aplysia* neurons (Tillotson, 1979).

Discussion

The major finding of the present study was that a Ca^{2+}-dependent inward current as well as Na^+ inward and K^+ outward currents could be identified in adult mammalian DRG cells. These three current systems could be separated according to their ionic selectivities, kinetic properties and pharmacological sensitivities. The peak current, the maximum conductance and the kinetic parameters of the ionic currents isolated in this study are summarized in the Table. Although complete isolation of the ionic currents was difficult, the kinetics of these currents were convincingly analyzed at least within a limited range of membrane potentials. Since the *cultured* DRG cells revealed a quite similar configuration of action potentials to that described for *in situ* and *dissected* mammalian DRG cells (Sato & Austin, 1961; Czéh, Kudo & Kuno, 1977; Yoshida, Matsuda & Samejima, 1978), it seems likely that similar ionic meachnisms also mediate the generation of the action potentials in these intact cells.

The Slow Calcium Current in Adult Mammalian Neurons

The slow inward current observed in Na^+-free solutions containing TEA and/or 4-AP has been identified as a Ca^{2+} current, which has essentially similar properties to those reported for many other neurons or tissues (for review, *see* Reuter, 1973; Hagiwara, 1975). The average value of 0.22 mA/cm^2 for the peak Ca^{2+} current density of the DRG neuron in 10 mM Ca^{2+}-containing solution was one order of magnitude smaller than the peak I_{Na}.

I_{Ca} is also smaller than I_K at 0 mV. This fact may be responsible for both the failure to elicit an active response in part of mouse DRG neurons in Na^+-free solution (Matsuda et al., 1976) and the appearance of a Ca^{2+}-dependent response in cat motoneurons following the addition of TEA or 4-AP (Barrett & Crill, 1980). It should also be mentioned that in the present study, I_{Ca} could be detected in almost all the adult cells in solutions containing both TEA and 4-AP.

Table. Summary of the properties of the ionic currents in DRG cells

Ion	Maximum peak current (mA/cm^2)	Maximum conductance (mS/cm^2)	Activation parameters		Inactivation parameters	
			$V_{\frac{1}{2}}$ (mV)	τ (ms)	$V_{\frac{1}{2}}$ (mV)	τ (ms)
Na	2.5	178	−17	0.16 at −8 mV	−60	0.86
K	0.57±0.25 (8) at 0 mV	26.1 ±8.9 (5)	13±4(5)	2.5±0.7(5)	–	10~ 50(5) 100~200(5)
Ca	0.22±0.14(11)	1.61±0.46(5)	−20±2(6)	2.6±0.5(5)	−38±5(5)	31± 17(7) 210~650(5)

$V_{\frac{1}{2}}$ is the potential for half activation or inactivation of each conductance. τ is the time constant at 0 mV unless otherwise stated. Values are given as means ±SD, with number of cells in parentheses, but for I_{Na} values are from one cell. Inactivation of I_K was not systematically analyzed. Temp.: 18~27 °C.

The kinetic parameters of I_{Ca} in the DRG cells could be determined at membrane potentials negative to 10 mV (Fig. 8). These values were in general agreement with those reported for internally perfused DRG cells except the time course of inactivation. It has been reported recently that the inactivation of I_{Ca} is governed by Ca^{2+} entry or the resultant elevation of $[Ca^{2+}]_i$ rather than a voltage-dependent process (Brehm & Ekert, 1978; Tillotson, 1979). In adult DRG cells, the slower time course of the Ba^{2+} current compared to I_{Ca} (Fig. 7) and the depressive effect of preceding pulses on I_{Ca} (Fig. 9) may provide support for Ca^{2+}-dependent inactivation of I_{Ca}, as found in chick embryonic DRG cells (Dunlap & Fischbach, 1981). Thus, the faster time course of inactivation of I_{Ca} compared to that in the internally perfused DRG cells may result from Ca^{2+}-dependent inactivation. It seems less likely, however, that all the steady-state inactivation of I_{Ca} is mediated by Ca^{2+}, since no inward current could be detected in the potential range of from −80 to −45 mV where part of the Ca^{2+} channels was apparently inactivated (h_∞ curve in Fig. 8). The results are more consistent with the idea that at least part of the inactivation of the Ca^{2+} channels is voltage-dependent.

Comparison with Embryonic and Neoplasmatic Neurons

The kinetic properties and pharmacological sensitivities of the Na^+, K^+ and Ca^{2+} currents in *adult* DRG cells are basically similar to those in chick *embryonic* DRG cells (Dunlap & Fischbach, 1981) and mouse neuroblastoma cells (Moolenaar & Spector, 1978). Although $\bar{g}_{Na}$ in the adult DRG cells seems to be comparable to that of neuroblastoma cells, $\bar{g}_K$ in the adult cells (26 mS/cm^2) is larger than that of neuroblastoma cells (12 mS/cm^2).

Furthermore, $\bar{g}_{Ca}$ in the adult cells appears to be smaller than that of embryonic DRG cells, since the largest I_{Ca} of 0.5 mA/cm^2 in embryonic cells (Dunlap & Fischbach, 1981) was larger than the corresponding value of 0.3 mA/cm^2 in the present study. $\bar{g}_{Ca}/\bar{g}_K$ in the adult membrane thus seems to be smaller than in embryonic membranes, although it is difficult to make a precise comparison at this time. A change in $\bar{g}_{Ca}/\bar{g}_K$ may account in part for the reduction of action potential duration during maturation of nerve cells as observed in mouse DRG cells (Matsuda et al., 1978; Yoshida et al., 1978).

Comparison with Mammalian Nodes of Ranvier

One of the most important differences in the ionic mechanisms between mammalian DRG somata and the nodes of Ranvier is that $\bar{g}_{Na}$ in the somata is 20-fold smaller than that in the nodes, suggesting a lower density of Na^+ channel in the somatic membranes. This idea may be supported by the finding (Richie & Rogart, 1977) that radiolabeled Saxitoxin binds to the rabbit node of Ranvier 22-fold more heavily than to the squid axon where a similar Na^+ current density to that of DRG cells has been found (Hodgkin & Huxley, 1952).

Another difference is that I_{Ca} has not been detected in the nodes of Ranvier. Although the functional significance of I_{Ca} in cell bodies remains unclear, it is of interest to speculate that I_{Ca} in the somatic membrane might play an important role in functions specific to the cell bodies, such as autorhythmic activity, metabolic control and initiation of axonal transport.

One more difference between the soma and the node is that $\bar{g}_K$ has been reported to be small or negligible in nodes of Ranvier (Nonner & Stämpfli, 1969; Chiu et al., 1979). Brismar (1980) has recently reported a maximum K^+ permeability of

2.1×10^{-4} cm/s (approximately 50 mS/cm^2) and a leak conductance of 130 mS/cm^2 in rat nodes. Thus, a $\bar{g}_K$ value in this range, if it exists, may not be very important for repolarization of action potentials in the mammalian node. On the other hand, $\bar{g}_K$ in the cell bodies is essential for repolarization of the action potential due to relatively small values of $\bar{g}_{Na}$ and the leak conductance. Indeed, application of TEA or 4-AP can significantly prolong the duration of the action potentials in DRG cell bodies (Funkuda & Kameyama, 1980*a*).

I would like to thank Prof. M. Ito and Dr. J. Fukuda for their constant advice and encouragement throughout this work. I also thank Profs. H. Irisawa and M. Morad for reading the manuscript. This work was carried out as partial fulfillment of the author's Ph. D. thesis.

References

Barrett, E.F., Barrett, J.N., Crill, W.E. 1980. Voltage sensitive outward current in cat motoneurons. *J. Physiol (London)* **304**:251–276

Barrett, J.N., Crill, W.E. 1980. Voltage clamp of cat motoneuron somata: Properties of the fast inward current. *J. Physiol. (London)* **304**:231–249

Brehm, P., Eckert, R.O. 1978. Calcium entry leads to inactivation of calcium channels in Paramecium. *Science* **202**:1203–1206

Brismar, T. 1980. Potential clamp analysis of membrane current in rat myelinated fibres. *J. Physiol. (London)* **298**:171–184

Chiu, S.Y., Ritchie, J.M., Rogart, R.B., Stagg, D. 1979. A quantitative description of membrane currents in rabbit myelinated nerve. *J. Physiol. (London)* **292**:149–166

Cole, K.S. 1968. Membranes, Ions and Impulses. University of California Press, Berkeley, Calif.

Czéh, G., Kudo, N., Kuno, M. 1977. Membrane properties and conduction velocity in sensory neurones following central or peripheral axotomy. *J. Physiol. (London)* **270**:165–180

Dunlap, K., Fischbach, G.D. 1981. Neurotransmitters decrease the calcium conductance activated by depolarization of embryonic chick sensory neurons. *J. Physiol. (London)* **317**:519–535

Fukuda, J., Fischbach, G.D., Smith, T.G., Jr. 1976. A voltage clamp study of the sodium, calcium and chloride spikes of chick skeletal muscle cells grown in tissue culture. *Dev. Biol.* **49**:412–424

Fukuda, J., Kameyama, M. 1979. Enhancement of Ca spikes in nerve cells of adult mammals during neurite growth in tissue culture. *Nature (London)* **279**:546–548

Fukuda, J., Kameyama, M. 1980*a*. Tetrodotoxin-sensitive and tetrodotoxin-resistant sodium channels in tissue-cultured spinal ganglion neurons from adult mammals. *Brain Res.* **182**:191–197

Fukuda, J., Kameyama, M. 1980*b*. A tissue-culture of nerve cells from adult mammalian ganglia and some electrophysiological properties of the nerve cells in vitro. *Brain Res.* **202**:249–255

Hagiwara, S. 1975. Ca-dependent action potential. *In:* Membranes, a Series of Advances. G Eisenman, editor. Vol. 3, pp. 359–382. Marcel Dekker, N.Y.

Hille, B. 1977. Ionic basis of resting and action potentials. *In:* Handbook of Physiology. E.R. Kandel, editor. Section 1: The nervous system. Chap. 4, pp. 99–136. Williams & Wilkins, Baltimore

Hodgkin, A.L., Huxley, A.F. 1952. A quantitative description of membrane current and its application to conduction and excitation in nerve. *J. Physiol. (London)* **117**:500–544

Kostyuk, P.G., Veselovsky, N.S., Fedulova, S.A. 1981. Ionic currents in the somatic membrane of rat dorsal root ganglion neurons–II. Calcium currents. *Neuroscience* **6**:2431–2437

Kostyuk, P.G., Veselovsky, N.S., Fedulova, S.A., Tsyndrenko, A.Y. 1981. Ionic currents in the somatic membrane of rat dorsal root ganglion neurons–III. Potassium currents. *Neuroscience* **6**:2439–2444

Kostyuk, P.G., Veselovsky, N.S., Tsyndrenko, A.Y. 1981. Ionic currents in the somatic membrane of rat dorsal root ganglion neurons–I. Sodium currents. *Neuroscience* **6**:2423–2430

Matsuda, Y., Yoshida, S., Yonezawa, T. 1976. A Ca-dependent regenerative response in rodent dorsal root ganglion cells cultured in vitro. *Brain Res.* **115**:334–338

Matsuda, Y., Yoshida, S., Yonezawa, T. 1978. Tetrodotoxin sensitivity and Ca component of action potentials of mouse dorsal root ganglion cells cultured in vitro. *Brain Res.* **154**:69–82

Moolenaar, W.H., Spector, I. 1977. Membrane currents examined under voltage clamp in cultured neuroblastoma cells. *Science* **196**:331–333

Moolenaar, W.H., Spector, I. 1978. Ionic currents in cultured mouse neuroblastoma cells under voltage-clamp conditions. *J. Physiol. (London)* **278**:265–286

Moolenaar, W.H., Spector, I. 1979. The calcium current and the activation of a slow potassium conductance in voltage-clamped mouse neuroblastoma cells. *J. Physiol. (London)* **292**:307–323

Nonner, W., Stämpfli, R. 1969. A new voltage clamp method. *In:* Laboratory Techniques in Membrane Biophysics. H. Passow and R. Stampfli, editors. pp. 171–175. Springer Verlag, Berlin

Rall, W. 1969. Time constant and electrotonic length of membrane cylinders and neurons. *Biophys. J.* **9**:1483–1508

Ransom, B.R., Holz, R.W. 1977. Ionic determinants of excitability in cultured mouse dorsal root ganglion and spinal cord cells. *Brain Res.* **136**:445–453

Ransom, B.R., Neale, E., Henkert, M., Bullock, P.N., Nelson, P.G. 1977. Mouse spinal cord in cell culture. I. Morphological and intrinsic neuronal electrophysiological properties. *J. Neurophysiol.* **40**:1132–1150

Reuter, H. 1973. Divalent cations as charge carriers in excitable membranes. *Prog. Biophys. Mol. Biol.* **20**:3–43

Ritchie, J.M., Rogart, R.B. 1977. Density of sodium channels in mammalian myelinated nerve fibers and nature of the axonal membrane under the myelin sheath. *Proc. Natl. Acad. Sci. USA* **74**:211–215

Sato, M., Austin, G. 1961. Intracellular potentials of mammalian dorsal root ganglion cells. *J. Neurophysiol.* **24**:569–582

Smith, T.G., Jr., Barker, J.L., Smith, B.M., Colburn, T.R. 1980. Voltage clamping with microelectrodes. *J. Neurosci. Methods* **3**:105–128

Tillotson, D. 1979. Inactivation of Ca conductance dependent on entry of Ca ions in molluscan neurons. *Proc. Natl. Acad. Sci. USA* **76**:1497–1500

Yoshida, S., Matsuda, Y., Samejima, A. 1978. Tetrodotoxin-resistant sodium and calcium component of action potentials in dorsal root ganglion cells of the adult mouse. *J. Neurophysiol.* **41**:1096–1106

Received 15 July 1982; revised 7 October 1982